

Frequency Offset Estimation and Correction

in the IEEE 802.11a WLAN

Essam Sourour, Hussein El-Ghoroury and Dale McNeill

Ellipsis Digital Systems, Inc., 6185 Paseo Del Norte, Suite 200, Carlsbad, CA 92009

sourour@ieee.org, hussein@ellipsisdigital.com, mcneill@ellipsisdigital.com

Abstract— This paper shows how to utilize the Short Training Sequence, Long Training Sequence and Pilot Subcarriers, of the IEEE 802.11a frame, to estimate and equalize the effect of both carrier and sampling frequency offset. To reduce cost the equalization process is performed digitally. Using computer simulation, we show that the presented scheme nearly eliminates the degradation due to frequency offset for all IEEE 802.11a modulation schemes. The performance measures are the root-mean-squared error (RMSE) and BER in a fading channel.

Keywords- OFDM, WLAN, frequency offset,, synchronization

I. INTRODUCTION

The IEEE 802.11a standard provides data rates up to 54 Mbps and is based on Orthogonal Frequency Division Multiplexing (OFDM) modulation [1]. OFDM is very sensitive to frequency offset [2] due to the local oscillator (LO) inaccuracy. The standard specifies the maximum LO offset to be ± 20 ppm of the carrier frequency. Frequency offset causes two phenomena at the receiver side, carrier frequency offset and sampling frequency offset. They both cause undesirable phase rotation to the OFDM subcarriers and create Inter-Carrier Interference (ICI). Many techniques have been proposed lately to estimate the frequency offset. Most of the techniques that are proposed for packet communications systems rely on the transmission of known training symbols at the beginning of the frame. Pilot symbols are also added within the payload for tracking purpose. In [2] and [3] a training symbol containing two identical halves is used for frequency offset estimation. Frequency estimation schemes are proposed in [4], [5] that rely on dividing the symbol into several identical shorter parts to increase the estimation range. In [6] a new training sequence is proposed which consists of identical parts with a sign change. The sign change is to improve time synchronization. The frequency offset estimation scheme in [6] is that of [4] with modifications to accommodate the sign change in the identical parts.

Very few papers presented a comprehensive utilization of the IEEE 802.11a frame structure for frequency offset estimation and the resulting performance at the different WLAN modulation schemes. In this paper we present a technique where coarse and fine frequency offset estimation is performed using the Short and the Long Training Sequences, respectively. Frequency offset tracking is performed using the Pilot Symbols embedded among the user data. We also investigate the improvement in frequency offset estimation when receiver antenna diversity is used. The frequency offset correction process is performed in the digital domain; i.e., the LO is not adjusted after frequency offset estimation. Using a

complete link simulation, we study the performance of the proposed technique in an IEEE 802.11a WLAN system.

II. IEEE 802.11a PHYSICAL LAYER

The IEEE802.11a WLAN is a packet communication system. As shown in Figure 1, the frame (packet) consists of two training sequences, designated Short Training (ST) and Long Training (LT), each with length 8 μ sec. These are followed by a train of OFDM Symbols of $T_u=4$ μ sec each. The ST is composed of 10 identical parts, denoted as t_0 to t_9 in Figure 1. Each part consists of 16 complex-valued samples [7]. The ST is mainly used for frame synchronization, Automatic Gain Control (AGC), antenna selection (in case of selection diversity), and coarse frequency offset estimation. In this paper we assume that synchronization has been achieved and frequency offset estimation is performed using the last 5 parts, t_5 to t_9 , only. The LT is composed of 2 identical parts, denoted as T_0 and T_1 in Figure 1, and a guard interval GI2. Each of T_0 and T_1 consists of 64 complex-valued. The guard interval GI2 consists of the last 32 samples of T_1 (cyclic prefix). Note that if the frame is subject to multipath fading with delay spread less than the duration of GI2, GI2 protects LT from ISI and the received T_0 and T_1 parts are still identical. The LT is mainly used for channel estimation and fine frequency offset estimation. Following the LT is a train of OFDM Symbols of 80 samples each. The last $N=64$ are the information carrying samples which are generated by an IFFT at the transmitter. The first $N_g=16$ samples are identical to the last 16 samples. These are used as guard interval which is denoted as GI in Figure 1. The first OFDM Symbol is the Signal Field, while the remaining OFDM Symbols are for the Data Field [7]. The Data field modulation is BPSK, QPSK, 16-QAM or 64-QAM. The frequency domain OFDM Symbol includes 4 pseudo-randomly generated ± 1 Pilot Symbols. The frequency domain OFDM Symbol is applied to a 64-point IFFT to produce the 64 information carrying samples.

III. CHANNEL AND FREQUENCY OFFSET MODELS

The results of this paper are based on a complete computer simulation of the transmitter, channel and receiver of the IEEE 802.11a WLAN system. The complex baseband samples of the frame are generated according to the standard. The frame samples are applied to a multipath fading channel, corrupted by Additive White Gaussian Noise (AWGN), and processed by the receiver. The RF front end of the actual receiver corrupts the received signal by frequency offset. In this section we describe how the fading channel and frequency offset are modeled in our simulation

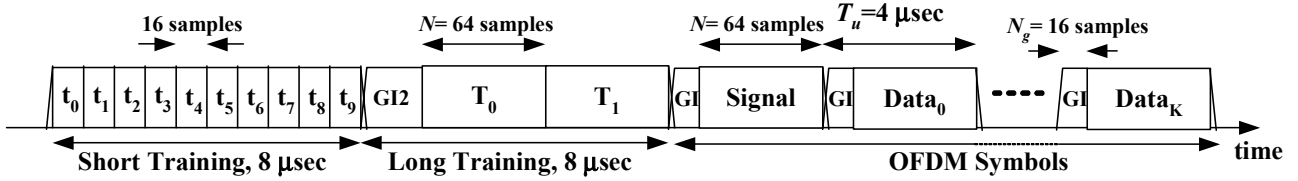


Figure 1, IEEE 802.11a frame structure

Channel Model:

We consider an indoor multipath Rayleigh faded channel model. The power delay profile is exponentially decaying with RMS delay spread in the range of $D_{rms} = 20$ to 200 nsec [9]. For simulation purpose, the number of channel paths is limited to $L = 1 + \lfloor 10D_{rms}/T_s \rfloor$, where T_s is the sampling period with the sampling performed at 20 MHz. The channel does not change during the frame duration. The channel impulse response is given by $h(t) = \sum_{l=0}^{L-1} g_l \delta(t - \tau_l)$, where g_l is a complex Gaussian random variable with zero mean and variance $\sigma_l^2 = \sigma_0^2 e^{-\tau_l/D_{rms}}$. For unity total channel power, the first path variance is given by $\sigma_0^2 = 1 - e^{-T_s/D_{rms}}$.

Frequency Offset Model:

In an actual receiver, the received signal is down-converted to baseband, filtered and sampled. The complex baseband samples are processed to extract the information bits. Down-conversion and sampling are derived from the same LO. Hence, the frequency offset of ϵ ppm is the same for carrier and sampling frequencies for all receiver antennas.

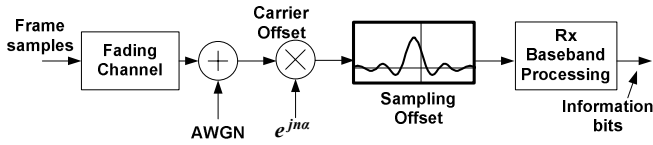


Figure 2, Modeling of carrier and sampling offset

A. Carrier Frequency Offset Modeling

The received frame at frequency f_c is down-converted with a local carrier frequency $(1+\epsilon)f_c$. The resulting baseband samples are subject to phase rotation. If ϵ is positive the phase rotation per sample, α , is also positive (counter-clockwise):

$$\alpha = 2\pi\epsilon f_c T_s \quad (1)$$

To model this effect, sample n of the received frame is multiplied by $e^{jn\alpha}$, as shown in Figure 2.

B. Sampling Frequency Offset Modeling

Due to sampling offset, the sampling duration is $T'_s = (1-\epsilon)T_s$. Hence, if the sampling ϵ offset is positive (negative) the n 'th sample in the frame is taken at time $\tau_n = n\epsilon T_s$ earlier (later) than it should. The upper part of Figure 3 shows an example with positive ϵ . The samples at ideal sampling points, S'_n , are shown with solid lines while the offset samples, S_n , are shown with dashed lines. To model the effect of sampling offset in the computer simulation we adjust the values of each complex sample to correspond to the offset sampling points. This process is performed digitally by applying the frame samples to a digital LPF with a *Sinc*

impulse response whose peak is at the offset sampling point. The Sync impulse response is sampled at locations $\tau_n + mT_s$, as shown in Figure 3. This is given by

$$C_m = \text{Sinc}(\pi(t + \tau_n)/T_s) \Big|_{t=mT_s}, \quad -\infty < m < \infty \quad (2)$$

$$= \text{Sinc}(\pi(m + n\epsilon))$$

For example, and referring to Figure 3, to generate the n 'th offset sample in the frame (S_n in the figure) we calculate the filter coefficient given by (2) and apply the ideal point frame samples as follows

$$S_n = \sum_{m=-\infty}^{\infty} C_m S'_{n+m} \quad (3)$$

In our simulation the LPF impulse response in (2) is limited to $-50 < m < 50$. Note that ideally the filter impulse response in (2) is different for each output sample. However, since ϵ is very small we can update the filter coefficients every OFDM Symbol (80 samples).

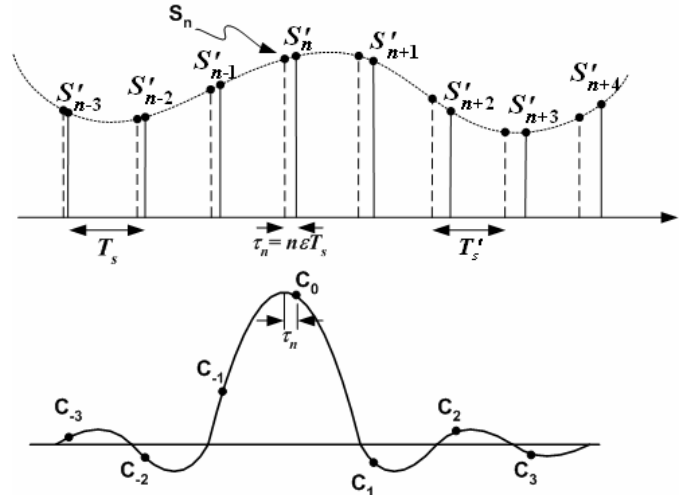


Figure 3, Calculating offset samples from the ideal samples

IV. FREQUENCY OFFSET ESTIMATION AND CORRECTION

Frequency offset estimation is performed using the ST, LT and the Pilot Symbols. The ST and LT are used, respectively, to calculate coarse and fine estimate of the phase rotation per sample, given by α in (1). The estimated value $\hat{\alpha}$ is used to multiply the baseband samples by $\exp(-jn\hat{\alpha})$ to compensate for the phase rotation due to carrier frequency offset. Since the LO frequency is not corrected, the sampling frequency offset still exists, which causes a phase rotation to OFDM symbols subcarriers after the receiver FFT [8]. We use $\hat{\alpha}$, together

with additional phase estimation using the Pilot Symbols, to correct for the resulting subcarrier phase rotation.

Estimation Using the Short Training:

As shown in Figure 1 the ST consists of 10 identical parts of 16 samples each. The last 5 parts are used for frequency offset estimation. For simplicity, Let us denote the ST complex samples of the last 5 parts as S_m , where $m=0,1, \dots, 79$. The coarse estimate of α is given by:

$$\hat{\alpha}_{ST} = \frac{1}{16} \angle \left(\sum_{m=0}^{63} S_m^* S_{m+16} \right), \quad (4)$$

$-\pi < \angle(z) \leq \pi$ is the phase of the complex variable z . Since $\alpha_{\max} < \pi/16$ there is no ambiguity in phase estimation in (4). The value of $\hat{\alpha}_{ST}$ is stored to be used in the next step.

Estimation and Correction Using the Long Training:

Referring to Figure 1, the two identical parts T_0 and T_1 of LT have 128 samples denoted here as S_m , $m=0,1, \dots, 127$. These samples are processed in 3 steps:

1. Coarse correction: the 128 samples are corrected as $S_m = S_m e^{-jm\hat{\alpha}_{ST}}$, $m=0, 1, \dots, 127$.
2. Fine estimation: the corrected samples are used for fine estimation as follows:

$$\hat{\alpha}_{LT} = \frac{1}{64} \angle \left(\sum_{m=0}^{63} S_m^* S_{m+64} \right). \quad (5)$$

3. Fine correction: the samples are corrected one more time as $S_m = S_m e^{-jm\hat{\alpha}_{LT}}$, $m=0, 1, \dots, 127$.

The final phase estimation $\hat{\alpha} = \hat{\alpha}_{ST} + \hat{\alpha}_{LT}$ is used for carrier frequency correction for the remaining part of the frame after LT. Correction starts from the first sample of the Signal field GI. Samples are multiplied by $\exp(-jn\hat{\alpha})$, where for phase continuity, the sample number n is started with $n=128$. The estimated phase $\hat{\alpha}$ is also used to find an initial estimate $\hat{\epsilon}_0$ of the frequency offset using (1).

Estimation and Correction Using the Pilot Symbols:

The identical LT parts, T_0 and T_1 are used for channel estimation. We denote the channel gain estimates as H_k , $k=-26$ to 26, where H_k is the complex channel gain for the k 'th subcarrier k . We denote the channel gains at the subcarrier locations $k=-21, -7, 7$ and 21 as $Q_{-2} = H_{-21}$, $Q_{-1} = H_{-7}$, $Q_1 = H_7$, and $Q_2 = H_{21}$. These locations correspond to the Pilot Symbols. The receiver baseband processing, is generally the reverse of the transmitter processing. For each OFDM Symbol the Guard Interval GI is dropped and the remaining 64 samples are applied to the FFT to generate the 48 Modulation Symbols and the 4 Pilot Symbols. After FFT, each Pilot symbol is multiplied by its corresponding pseudo-random value to remove the randomness. With the Pilot Symbols randomness removed, the FFT output is denoted as $X_{l,k}$, where k is the subcarrier number, $k=-26$ to 26, and l is the OFDM Symbol number starting from $l=1$ at the Signal field. For simple notation we always refer to the Pilot Symbols at the l 'th OFDM Symbol as $P_{l,-2}, P_{l,-1}, P_{l,1}, P_{l,2}$, and

$P_{l,2} = X_{l,21}$. In the presence of residual frequency offset and sampling frequency offset the FFT outputs, including the Pilot Symbols, will incur phase rotation. The Pilot Symbols $P_{l,i}$ and the corresponding channel gains Q_i , $i=-2, -1, 1, 2$, are used to estimate this offset.

We briefly describe the effect of frequency offset on the output of the FFT. It is shown in [8] that the output $X_{l,k}$ of the FFT includes the desired part, ICI and AWGN. Focusing on the desired part, it is shown that due to frequency offset, each FFT output $X_{l,k}$ incurs extra phase rotation $\phi_{l,k}$ given by

$$\phi_{l,k} = 2\pi l \left(\epsilon_r T_u f_c - \frac{N + N_g}{N} \epsilon k \right). \quad (6)$$

Contrary to [18], positive ϵ means faster sampling. Hence, the second term is negative. In the above equation $N=64$ is the FFT size, $N_g=16$ is the number of samples in GI, $T_u=4$ μ sec is the OFDM Symbol duration in time domain and $\epsilon_r = \epsilon - \hat{\epsilon}_0$ is the residual carrier frequency offset after LT correction, which is nonzero if $\hat{\alpha} \neq \alpha$. The first part in the right hand side of (6) is due to the residual carrier frequency offset not corrected after LT correction. This term is equal for all subcarriers of the same OFDM Symbol. The second part is due to the continuous drift in the sampled waveform of the OFDM Symbol due to sampling offset. This phase depends linearly on the subcarrier number. It is implied in (6) that the phase of the channel gain H_k is the reference. To correct for the two offsets we propose a 3 steps method to be applied for each OFDM Symbol as follows. 1) Correct sampling offset, 2) Correct residual carrier frequency offset, and 3) Finer frequency offset estimation $\hat{\epsilon}_l$, $l \geq 1$, to be used in subsequent sampling offset corrections. The 3 steps are explained below.

1. Correct Sampling Frequency Offset

For the l 'th OFDM Symbol at the output of the FFT we first compensate for the second term in the right hand side of (6). Using the available frequency offset estimate $\hat{\epsilon}_{l-1}$ the l 'th OFDM Symbol FFT output is updated as:

$$X_{l,k} = X_{l,k} \exp \left(2\pi l \frac{N + N_g}{N} \hat{\epsilon}_{l-1} k \right), \quad k=-26, \dots, 26 \quad (7)$$

Note that this correction includes the Pilot Symbols $P_{l,i}$. When processing the Signal field ($l=1$) the value of $\hat{\epsilon}_0$ is the one generated from the LT processing. As more OFDM Symbols are received the frequency offset estimate $\hat{\epsilon}_l$ improves.

2. Correct Residual Carrier Frequency Offset

We now switch attention to the first term in the right hand side of (6). This term, is due to the accumulated phase rotation, at the l 'th OFDM Symbols, when $\hat{\alpha} \neq \alpha$. This rotation is the same for all subcarriers. A good estimate of it is given by

$$\hat{\beta}_l = \angle \left(\sum_{i=-2,-1,1,2} P_{l,i} Q_i^* \right). \quad (8)$$

Now the output of (7) is corrected one more time as follows.

$$X_{l,k} = X_{l,k} e^{-\hat{\beta}_l}, \quad k = -26, \dots, 26, \quad k \neq -21, -7, 7, 21 \quad (9)$$

The correction performed by (9) attempts to remove the phase rotation completely from all Modulation Symbols. However, the Pilot Symbols are not corrected since they will be used in the next step for finer estimation of the frequency offset estimate $\hat{\epsilon}_l$. At this point the output of the FFT is ready for channel equalization and the receiver processing.

3. Fine estimation of Frequency Offset

Our goal is to improve the estimate $\hat{\epsilon}_l$ to be used in step 1 for the following OFDM Symbol. The approach we use is based on the observation that the actual frequency offset ϵ is given by the sum of the initial estimate, performed at LT processing, and the residual component, i.e., $\epsilon = \hat{\epsilon}_0 + \epsilon_r$. The residual component is the source of the first phase rotation term in (6). This term is corrected in step 2 for the Modulation Symbols at the output of the FFT. However, the Pilot Symbols are not corrected and can be used to estimate the residual frequency offset. We first calculate the variable W_l as follows

$$W_l = \sum_{i=-2,-1,1,2} P_{l,i} P_{l-1,i}^* \quad (10)$$

From (6) and (10), we notice that $\angle(W_l)$ is an estimate of the phase increment $2\pi\epsilon_r T_w f_c$, over one OFDM Symbol, due to the residual carrier frequency offset. For $l=1$, we set $P_{0,i} = Q_i$. To improve the accuracy of estimation we could continuously accumulate W_l every new OFDM Symbol. However, continuous addition would be problematic in a fixed-point hardware implementation. As a trade off we add groups of 4 successive values and exponentially filter the sum. At OFDM Symbols numbers $l = 4, 8, 12, 16, \dots$ we add the latest 4 values of W_l and filter the sum as follows:

$$\text{Addition: } V_l = \sum_{m=l-3}^l W_m \quad (11)$$

$$\text{Filtering: } U_l = \rho V_l + (1-\rho)U_{l-4} \quad (12)$$

The parameter ρ is taken to be 1/32. Every 4th OFDM Symbol a filtered value U_l is generated, and a corresponding new estimates ϵ_r and $\hat{\epsilon}_l$ are updated as follows:

$$\hat{\epsilon}_r = \angle(U_l) / (2\pi T_w f_c) \quad , \quad l = 4, 8, 12, 16, \dots \quad (13)$$

$$\hat{\epsilon}_{l+1} = \hat{\epsilon}_{l+2} = \hat{\epsilon}_{l+3} = \hat{\epsilon}_l = \hat{\epsilon}_0 + \hat{\epsilon}_r \quad , \quad l = 4, 8, 12, 16, \dots \quad (14)$$

V. ANTENNA DIVERSITY UTILIZATION

Antenna diversity improves the BER performance in fading channels, regardless of frequency offset. We can also improve frequency offset estimation with antenna diversity. We consider two independently fading receiving antennas. It is assumed that both antennas derive their clocks from the same LO source at the receiver. Hence, the frequency offset is the same. We consider antenna selection and combining.

Antenna Selection

Antenna selection is based on the received signal power during the first 5 ST parts. Once an antenna is selected, all the

processing described before is performed using the signal from the selected antenna. To focus on the issue at hand in this paper we do not consider error in antenna selection.

Antenna Combining

Antenna combining yields a better performance than selection. To benefit from antenna combining we combine the results from two antennas. Hence, with two antennas, the phase estimates $\hat{\alpha}_{ST}$ and $\hat{\alpha}_{LT}$ (4) and (5) are changed to:

$$\hat{\alpha}_{ST} = \frac{1}{16} \angle \left[\overbrace{\sum_{m=0}^{63} S_m^* S_{m+16}}^{\text{first antenna}} + \overbrace{\sum_{m=0}^{63} S_m^* S_{m+16}}^{\text{second antenna}} \right] \quad , \quad (15) \text{ and}$$

$$\hat{\alpha}_{LT} = \frac{1}{64} \angle \left[\overbrace{\sum_{m=0}^{63} S_m^* S_{m+64}}^{\text{first antenna}} + \overbrace{\sum_{m=0}^{63} S_m^* S_{m+64}}^{\text{second antenna}} \right] \quad , \quad (16)$$

The combined estimates are used to find the fine phase estimate $\hat{\alpha} = \hat{\alpha}_{ST} + \hat{\alpha}_{LT}$ which is used for both antennas. The corresponding frequency offset $\hat{\epsilon}_0$ will be used in (7) for sampling frequency offset correction. In addition, we improve the estimation of the residual frequency offset by replacing (8) and (10), respectively, by

$$\hat{\beta}_l = \angle \left[\overbrace{\sum_{i=-2,-1,1,2} P_{l,i} Q_i^*}^{\text{first antenna}} + \overbrace{\sum_{i=-2,-1,1,2} P_{l,i} Q_i^*}^{\text{second antenna}} \right] \quad , \quad (17) \text{ and}$$

$$W_l = \overbrace{\sum_{i=-2,-1,1,2} P_{l,i} P_{l-1,i}^*}^{\text{first antenna}} + \overbrace{\sum_{i=-2,-1,1,2} P_{l,i} P_{l-1,i}^*}^{\text{second antenna}} \quad (18)$$

The value of W_l given by (18) is used in (11) and the resulting estimate new estimate $\hat{\epsilon}_r$ in (13) is used as explained before.

VI. NUMERICAL RESULTS

A computer simulation for the IEEE 802.11a WLAN is used to verify the frequency offset estimation technique described in this paper. We assume a carrier frequency $f_c=5$ GHz, sampling frequency $f_s=20$ MHz and an initial frequency offset of $\epsilon=40$ ppm. The fading channel RMS delay spread is $D_{RMS}=100$ nsec and the number of bytes per frame is 1000. The performance measure is the frequency estimation RMSE and channel BER (i.e., before the decoder). The RMSE is defined

by $RMSE = \sqrt{\frac{1}{F} \sum_F (\epsilon - \hat{\epsilon}_0)^2}$, where F is the number of

simulated frames, which we take as $F=40,000$. The RMSE is plotted versus the SNR per subcarrier (SNR_c). The channel BER is plotted versus the channel bits E_b/N_0 which is given by $SNR_c S/M$, where M is the modulation index and $S=2$ for the case of antenna combining and $S=1$ otherwise.

Figure 4 shows the RMSE after ST processing and after LT processing. For the RMSE after ST processing we use the estimate $\hat{\alpha}_{ST}$ to calculate $\hat{\epsilon}_0$ using (1), while for the RMSE

after LT we use $\hat{\alpha} = \hat{\alpha}_{ST} + \hat{\alpha}_{LT}$. It can be seen in this figure that the LT processing improves the estimation of the ST reasonably. Also, antenna selection or combining diversity provides reasonable improvement. Figure 5 shows the improvement in estimation when Pilot Symbols of successive OFDM Symbols are used after ST+LT processing. It can be seen that RMSE is reduced rapidly in the first 50 OFDM Symbols and slowly afterwards. At SNR_c of 6 dB the RMSE is below 0.2 ppm after 50 OFDM Symbols.

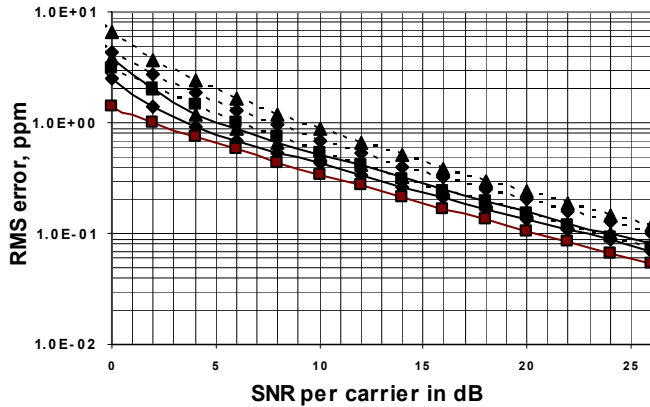


Figure 4, RMS error after ST and LT processing. Dashed line: After ST Processing, Solid line: After LT Processing. In each group, from upper to lower: Single Antenna, Selection Diversity then Combining Diversity

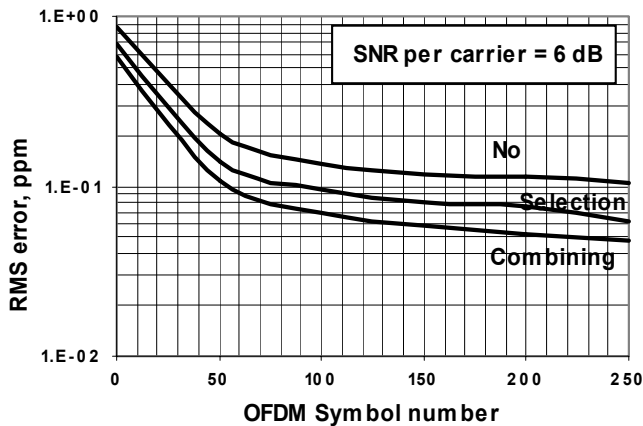


Figure 5, RMS error after Pilot Symbol processing

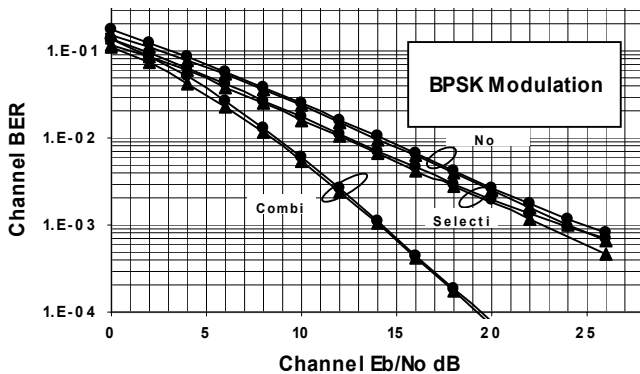


Figure 6, Channel BER for Configuration 1 (BPSK)

The channel BER is shown in Figure 6 and Figure 7, respectively, for BPSK and 64-QAM modulation schemes. The QPSK modulation provided similar results to the BPSK. It can be seen in the three figures that the degradation due to carrier and sampling frequency offset is negligible in all cases of modulation and diversity schemes.

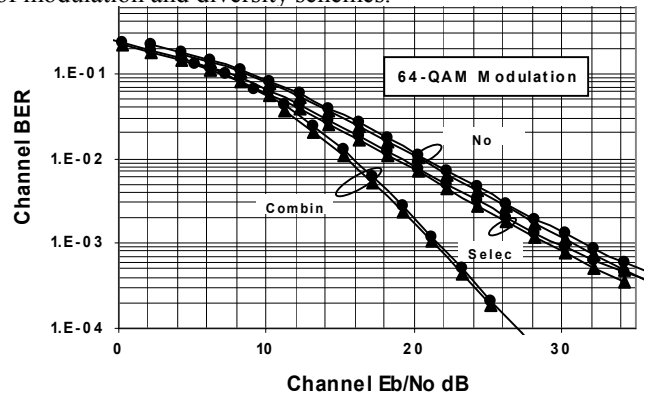


Figure 7, Channel BER for Configuration 8 (64-QAM)

REFERENCES:

- [1] R. van Nee, G. Awater, M. Morikura, H. Takanashi, M. Webster, and K. Halford, "New high-rate wireless LAN standards," *IEEE Comm. Mag.*, vol. 37, pp. 82–88, Dec. 1999.
- [2] Thomas Keller and Lajos Hanzo, "Adaptive Multicarrier Modulation: A Convenient Framework for Time-Frequency Processing in Wireless Communications," *Proceedings of the IEEE*, Vol. 88, No. 5, pp. 611–640, May 2000
- [3] T. M. Schmidl and D. C. Cox, "Robust frequency and timing synchronization for OFDM," *IEEE Trans. Comm.*, vol. 45, pp. 1613–1621, Dec. 1997.
- [4] M. Morelli and U. Mengali, "An improved frequency offset estimator for OFDM applications," *IEEE Comm. Lett.*, vol. 3, pp. 75–77, Mar. 1999.
- [5] Hyoun-Kyu Song, Young-Hwan You, Jong-Ho Paik, and Yong-Soo Cho, "Frequency-Offset Synchronization and Channel Estimation for OFDM-Based Transmission," *IEEE Comm. Lett.*, vol. 4, No. 3, pp. 95–97, March 2000..
- [6] Hlaing Minn, Vijay K. Bhargava, and Khaled Ben Letaief, "A robust timing and frequency synchronization for OFDM systems," *IEEE Trans. Wireless Comm.*, Vol. 2, No. 4, pp. 822–839, July 2003.
- [7] IEEE Std 802.11a/D7.0-1999, "Part11: Wireless LAN Medium Access Control (MAC) and Physical Layer (PHY) Specifications: High Speed Physical Layer in the 5GHz Band.
- [8] Michael Speth, Stefan A. Fechtel, Gunnar Fock, and Heinrich Meyr, "Optimum receiver design for wireless broad-band systems using OFDM—Part I," *IEEE Trans. Comm.*, vol. 47, No. 11, pp. 1668–1677, Nov. 1999.
- [9] R. van Nee and R. Prasad, *OFDM for Wireless Multimedia Communications*. Norwood, MA: Artech, 2000